Inorg. Chem. **2009**, *48*, 3274−3286

Substitution and Reaction Chemistry of Cobalt Complexes Supported by $[N_2P_2]$ Ligands

Wayne A. Chomitz and John Arnold*

Department of Chemistry, University of California, Berkeley, California 94720-1460

Received December 6, 2008

The coordination chemistry of mono- and divalent cobalt complexes supported by the monoanionic multidentate ligands, $[N_2P_2]$ (where $[N_2P_2] = {}^{t}BuN^{(-)}SiMe_2N(CH_2CH_2P^{i}Pr_2)_2$) and $[N_2P_2^{tolyl}]$ (where $[N_2P_2^{tolyl}] = MeC_6H_4N^{(-)}SiMe_2(CH_2CH_2P^{i}Pr_2)_2$), is presented. The Co(II) halide complex $[N_2P_2]CoI$ (**2**) serves as a precursor to the alkyl, hydride, and amide species $[N_2P_2]CoMe$ (**3**), $[N_2P_2]CoCH_2SiMe_3$ (**4**), $[N_2P_2]CoH$ (**5**), $[N_2P_2]CoNHPh$ (**10**), and $[N_2P_2]CoNHC_6H_4Me$ (**11**). Reduction of **2** results in the formation of a stable, monomeric Co(I) species, $[N_2P_2]Co$ (**6**). Compound **6** can be trapped with CO to form either $[N_2P_2]Co(CO)$ (**7**) or $[{}^{t}BuN(C{=}O)SiMe_2N(CH_2CH_2P^{i}Pr_2)_2]Co(CO)_2$ (**8**) depending on the number of equivalents of CO introduced. Compound **6** also serves as a precursor to transient Co(III) imido species. The Co(II) halide complex $[N_2P_2^{tolyl}]CoI$ (**16**) is synthesized through an analogues reaction to that of **2**. Reduction of **16** results in the formation of $[N_2P_2^{tolyl}]Co$ (**17**), and differences in the coordination and reaction chemistry of **6** and **17** are described.

Introduction

Numerous advances in reaction chemistry have resulted from the development of ligand scaffolds capable of engendering new and unusual reactivity at metal centers. These include the isolation of middle-to-late transition metal complexes containing metal−ligand multiple bonds such as terminal metal-oxos,[1−4] metal-imidos,[5−18] and metal-nitrides.[19−21] Metal-imido complexes are of particular interest given their role in hydroamination[22] and C−H bond activation,[23−25] in addition to acting as isoelectronic analogues to oxo functionalities.

The synthesis of late first-row transition metal imides frequently involves the addition of alkyl- or arylazide to a low-valent metal complex followed by reduction of azide, releasing N_2. Over the past few years, our group has examined the utility of tetradenate monoanionic ligands (TDMA) for stabilizing reactive complexes that exhibit interesting and unusual chemistry.[26−30] Recently we reported the synthesis and reduction chemistry of a number of first-row transition metal complexes supported by the monoanionic multidentate $[N_2P_2]$ ligand, where $[N_2P_2] = [{}^{t}BuN^{(-)}SiMe_2N(CH_2CH_2P^{i}Pr_2)_2]$. This work demonstrated how hemilabile ligands such as $[N_2P_2]$ could be used to stabilize unusual metal−ligand bonds such as bridging dinitrogen moieties on a range of transition metals, as well as showing that the $[N_2P_2]$ ligand was capable of stabilizing low-valent first-row metal complexes.

Given the promising nature of our initial results, we wished to extend this work with the aim of synthesizing compounds exhibiting reactive metal−ligand multiple bonds, whose subsequent reactivity with small molecules could be probed. To establish a well-behaved system on which to expand, Co(III) imidos were initially targeted because they are typically low-spin, allowing for characterization by NMR spectroscopy.[6,8,9,11] Though group transfer reactions by first-row metal imido complexes have been observed,[5,10−12,14] the results with Co have been limited. Interestingly, however, spin-crossover behavior leading to intramolecular C−H activation has been observed.[16,17]

Here we report on our results on the synthesis and characterization of a range of organometallic and reduced metal species that establish the versatility of the $[N_2P_2]$ ligand set for stabilizing a range of potentially useful starting materials. Work toward supporting transient Co(III) imido species which undergo H-atom abstraction and nitrene group transfer reactions is also described. Some of these results have been communicated in preliminary form.[27]

Experimental Section

All reactions were performed using standard Schlenk-line techniques or in an MBraun drybox (<1 ppm O_2/H_2O) unless noted otherwise. All glassware, cannulae, and Celite were stored in an

* To whom correspondence should be addressed. E-mail: arnold@berkeley.edu.

10.1021/ic802337t CCC: $40.75
Published on Web 03/04/2009

Table 1. Physical Properties of **2**−**12** and **16**−**18**

compound number	compound name	color	M.P. (°C)	yield (%)	μ_{eff} (μ_B)	coordination mode
2	$[N_2P_2]CoI$	green	173−174	83	4.0	κ^3-NP_2
3	$[N_2P_2]CoMe$	green	(dec) 140	53	1.8	κ^4-N_2P_2
4	$[N_2P_2]CoCH_2SiMe_3$	lime-green	74−76	57	4.2	κ^3-N_2P
5	$[N_2P_2]CoH$	olive-green	135−136	69	2.0	κ^4-N_2P_2
6	$[N_2P_2]Co$	blue	126−128	84	3.0	κ^4-N_2P_2
7	$[N_2P_2]Co(CO)$	green	151−152	54	3.0	κ^3-NP_2
8	$[^tBuN(C{=}O)SiMe_2N(CH_2CH_2P^iPr_2)_2]Co(CO)_2$	yellow	(dec) 115−117	80		
9	$[N_2P_2]CoBr$	green	199−200	53	4.1	κ^3-NP_2
10	$[N_2P_2]CoNHC_6H_5$	red-orange	99−101	72	3.8	κ^3-N_2P
11	$[N_2P_2]CoNHC_6H_5CH_3$	red	105−107	73	4.1	κ^3-N_2P
12	$[PhN{=}P^iPr_2(CH_2)_2NPh]$ $[^tBuNHSiMe_2N(CH_2)_2P^iPr_2]Co$	lime-green	132−135	1−15	4.1	
16	$[N_2P_2^{tolyl}]CoI$	brown	208−209	80	4.2	κ^3-NP_2
17	$[N_2P_2^{tolyl}]Co$	green	85−87	72	3.0	κ^4-N_2P_2
18	$[N_2P_2^{tolyl}]Co(CO)$	red	162−163	43	2.8	

oven at >425 K. Pentane, toluene, diethyl ether, and tetrahydrofuran were purified by passage through a column of activated alumina and degassed with nitrogen prior to use.[31] Deuterated solvent was vacuum transferred from sodium/benzophenone (benzene). NMR spectra were recorded at ambient temperature on Bruker AV-300, AVQ-400, AVB-400, and DRX-500 spectrometers. ^1H and $^{13}C\{^1H\}$ chemical shifts are given relative to residual solvent peaks, and coupling constants (J) are given in hertz. $^{31}P\{^1H\}$ chemical shifts are referenced to an external standard of $P(OMe)_3$ set to 1.67 ppm. Infrared samples were prepared as Nujol mulls and taken between KBr disks. Magnetic susceptibility (μ_{eff}) values were determined using the solution Evans method at ambient temperature (22 °C).[32] Melting points were determined using sealed capillaries prepared under nitrogen and are uncorrected. $Li[N_2P_2]$,[28] $[N_2P_2]CoCl$ (**1**),[28] phenylazide,[33] and *p*-tolylazide[33] were prepared using the literature procedures, and unless otherwise noted all reagents were acquired from commercial sources. Elemental analyses and mass spectral data were determined at the College of Chemistry, University of California, Berkeley. The X-ray structural determination was performed at CHEXRAY, University of California, Berkeley. A full list of compounds and their physical properties is provided in Table 1.

$[N_2P_2]CoI$ (2). A solution of $Li[N_2P_2]$ (4.00 g, 9.08 mmol) in 50 mL of toluene was added to a suspension of CoI_2 (2.83 g, 9.07 mmol) in 50 mL of toluene at −70 °C. The reaction mixture was warmed to room temperature and was stirred overnight. The resulting dark green solution was filtered, and the remaining solid was washed with 30 mL of toluene. The combined filtrates were concentrated and stored at −40 °C overnight, resulting in the formation of dark green crystals in 83% yield (4.66 g). ^1H NMR (C_6D_6): δ 0.25 (s); 1.09 (s); 1.18 (s); 2.12 (s); 3.09 (s); 3.25 (s); 4.13 (s); 4.78 (br s); 8.74 (br s); 23.27 (br s). IR (cm^{-1}): 1410 (w); 1350 (w); 1306 (w); 1245 (s); 1198 (s); 1105 (m); 969 (w); 926 (m); 884 (w); 845 (s); 797 (m); 760 (m); 738 (s); 696 (w); 655 (s); 602 (w); 532 (w); 478 (m). Anal. Calcd for $C_{22}H_{51}CoIN_2P_2Si$: C: 42.64; H: 8.31; N: 4.52. Observed. C: 42.86; H: 8.37; N, 4.85. mp = 173−174 °C. μ_{eff} = 4.0 μ_B.

$[N_2P_2]CoMe$ (3). Methyl lithium (1.6 M in Et_2O, 0.45 mL, 0.71 mmol) was added to a suspension of **2** (0.40 g, 0.64 mmol) in 10 mL of Et_2O at −70 °C. The reaction mixture was warmed to room temperature and was stirred overnight. Following the removal of solvent under vacuum, the crude product was extracted with pentane. Following concentration and cooling at −40 °C, dark green crystals were isolated in 53% yield (0.17 g). ^1H NMR (300 MHz, C_6D_6): δ −30.58 (br s); −1.52 (br s); −0.65 (br s); 1.17 (m); 2.28 (br s); 5.69 (br s); 10.56 (br s); 12.05 (br s); 17.86 (br s); 31.17 (br s); 35.19 (br s); 41.89 (br s). IR (cm^{-1}): 1344 (m); 1239 (m); 1215 (m); 1200 (s); 1087 (m); 1039 (m); 1018 (w); 909 (w); 882 (m);

(1) Klinker, E. J.; Kaizer, J.; Brennessel, W. W.; Woodrum, N. L.; Cramer, C. J.; Que, L. *Angew. Chem., Int. Ed.* **2005**, *44*, 3690–3694.
(2) MacBeth, C. E.; Golombek, A. P.; Young, V. G.; Yang, C.; Kuczera, K.; Hendrich, M. P.; Borovik, A. S. *Science* **2000**, *289*, 938–941.
(3) MacBeth, C. E.; Gupta, R.; Mitchell-Koch, K. R.; Young, V. G.; Lushington, G. H.; Thompson, W. H.; Hendrich, M. P.; Borovik, A. S. *J. Am. Chem. Soc.* **2004**, *126*, 2556–2567.
(4) Rohde, J. U.; In, J. H.; Lim, M. H.; Brennessel, W. W.; Bukowski, M. R.; Stubna, A.; Munck, E.; Nam, W.; Que, L. *Science* **2003**, *299*, 1037–1039.
(5) Bart, S. C.; Lobkovsky, E.; Bill, E.; Chirik, P. J. *J. Am. Chem. Soc.* **2006**, *128*, 5302–5303.
(6) Betley, T. A.; Peters, J. C. *J. Am. Chem. Soc.* **2003**, *125*, 10782–10783.
(7) Brown, S. D.; Peters, J. C. *J. Am. Chem. Soc.* **2005**, *127*, 1913–1923.
(8) Cowley, R. E.; Bontchev, R. P.; Sorrell, J.; Sarracino, O.; Feng, Y. H.; Wang, H. B.; Smith, J. M. *J. Am. Chem. Soc.* **2007**, *129*, 2424.
(9) Dai, X. L.; Kapoor, P.; Warren, T. H. *J. Am. Chem. Soc.* **2004**, *126*, 4798–4799.
(10) Hu, X. L.; Meyer, K. *J. Am. Chem. Soc.* **2004**, *126*, 16322–16323.
(11) Jenkins, D. M.; Betley, T. A.; Peters, J. C. *J. Am. Chem. Soc.* **2002**, *124*, 11238–11239.
(12) Kogut, E.; Wiencko, H. L.; Zhang, L. B.; Cordeau, D. E.; Warren, T. H. *J. Am. Chem. Soc.* **2005**, *127*, 11248–11249.
(13) Lu, C. C.; Saouma, C. T.; Day, M. W.; Peters, J. C. *J. Am. Chem. Soc.* **2007**, *129*, 4–5.
(14) Mindiola, D. J.; Hillhouse, G. L. *J. Am. Chem. Soc.* **2001**, *123*, 4623–4624.
(15) Nieto, I.; Ding, F.; Bontchev, R. P.; Wang, H.; Smith, J. M. *J. Am. Chem. Soc.* **2008**, *130*, 2716.
(16) Shay, D. T.; Yap, G. P. A.; Zakharov, L. N.; Rheingold, A. L.; Theopold, K. H. *Angew. Chem., Int. Ed.* **2005**, *44*, 1508–1510.
(17) Shay, D. T.; Yap, G. P. A.; Zakharov, L. N.; Rheingold, A. L.; Theopold, K. H. *Angew. Chem., Int. Ed.* **2006**, *45*, 7870–7870.
(18) Thomas, C. M.; Mankad, N. P.; Peters, J. C. *J. Am. Chem. Soc.* **2006**, *128*, 4956–4957.
(19) Betley, T. A.; Peters, J. C. *J. Am. Chem. Soc.* **2004**, *126*, 6252–6254.
(20) Scepaniak, J.; Fulton, M. D.; Bontchev, R. P.; Duesler, E. N.; Kirk, M. L.; Smith, J. M. *J. Am. Chem. Soc.* **2008**, *130*, 10515.
(21) Vogel, C.; Heinemann, F. W.; Sutter, J.; Anthon, C.; Meyer, K. *Angew. Chem., Int. Ed.* **2008**, *47*, 2681–2684.
(22) Pohlki, F.; Doye, S. *Chem. Soc. Rev.* **2003**, *32*, 104–114.
(23) Walsh, P. J.; Hollander, F. J.; Bergman, R. G. *J. Am. Chem. Soc.* **1988**, *110*, 8729–8731.
(24) Cummins, C. C.; Baxter, S. M.; Wolczanski, P. T. *J. Am. Chem. Soc.* **1988**, *110*, 8731–8733.
(25) Dewith, J.; Horton, A. D. *Angew. Chem., Int. Ed.* **1993**, *32*, 903–905.
(26) (a) Chomitz, W. A.; Arnold, J. *Chem. Commun.* **2007**, 4797–4799. (b) Chomitz, W. A.; Arnold, J. *Dalton Trans.* **2009**, 1714–1720. (c) Chomitz, W. A.; Arnold, J. *Chem. Eur. J.* **2009**, *15*, 2020–2030.
(27) Chomitz, W. A.; Arnold, J. *Chem. Commun.* **2008**, 3648–3650.
(28) Chomitz, W. A.; Mickenberg, S. F.; Arnold, J. *Inorg. Chem.* **2008**, *47*, 373–380.
(29) Chomitz, W. A.; Minasian, S. G.; Sutton, A. D.; Arnold, J. *Inorg. Chem.* **2007**, *46*, 7199–7209.
(30) Westmoreland, I.; Arnold, J. *Dalton Trans.* **2006**, 4155–4163.
(31) Alaimo, P. J.; Peters, D. W.; Arnold, J.; Bergman, R. G. *J. Chem. Educ.* **2001**, *78*, 64–64.
(32) Piguet, C. *J. Chem. Educ.* **1997**, *74*, 815–816.
(33) Murata, S.; Abe, S.; Tomioka, H. *J. Org. Chem.* **1997**, *62*, 3055–3061.

848 (s); 788 (m); 753 (m); 729 (m); 678 (w); 651 (m); 530 (w); 484 (w). Anal. Calcd $C_{23}H_{54}CoN_2P_2Si$. C: 54.48; H: 10.76; N: 5.53. Observed. C: 54.73; H: 11.09; N: 5.48. mp (dec) = 140 °C. μ_{eff} = 1.8 μ_B.

[N_2P_2]CoCH$_2$SiMe$_3$ (4). A solution of $LiCH_2SiMe_3$ (0.046 g, 0.48 mmol) in 5 mL of THF was added to a solution of **2** (0.30 g, 0.48 mmol) in 5 mL of THF at −40 °C. The reaction mixture was allowed to warm to room temperature and was stirred overnight. The solvent was removed under vacuum, and the crude product was extracted with pentane. Following concentration and cooling at −40 °C, green crystals were isolated in 57% yield (0.16 g). ^{1}H NMR (300 MHz, C_6D_6): δ −53.97 (br s); −44.93 (br s); −34.37 (br s); −30.85 (br s); −7.68 (br s); −6.61 (br s); −5.55 (br s); 0.01 (s); 0.036 (s); 1.08 (m); 3.93 (br s); 4.97 (br s); 13.72 (br s); 18.59 (br s); 28.68 (br s); 33.49 (br s); 39.49 (br s); 41.54 (br s); 96.18 (br s); 103.93 (br s). IR (cm^{-1}): 1348 (m); 1292 (w); 1233 (s); 1174 (m); 1076 (s); 1056 (s); 1037 (m); 923 (w); 882 (s); 845 (s); 817 (s); 791 (m); 769 (m); 738 (m); 719 (m); 687 (w); 667 (m); 642 (w); 608 (m); 537 (w); 521 (m); 490 (w); 459 (w). Anal. Calcd $C_{26}H_{62}CoN_2P_2Si_2$. C: 53.84; H: 10.80; N: 4.83. Observed. C: 53.79; H: 11.12; N: 4.81. mp = 74−76 °C. μ_{eff} = 4.2 μ_B.

[N_2P_2]CoH (5). *N*-butyl lithium (1.6 M in hexanes, 0.30 mL, 0.48 mmol) was added to a solution of **2** (0.30 g, 0.48 mmol) in 5 mL of THF at −40 °C. The cold bath was removed, and the reaction mixture was allowed to warm to room temperature and was stirred for 3 h. Following the removal of solvent under vacuum, the crude product was extracted with pentane. The resulting solution was concentrated and cooled at −40 °C overnight, resulting in the isolation of olive green crystals in 69% yield (0.16 g). ^{1}H NMR (300 MHz, C_6D_6): δ −30.52 (br s); −1.78 (br s); −0.58 (br s); 1.11 (m); 2.05 (s); 5.69 (s); 12.05 (br s); 17.91 (br s); 31.18 (br s); 35.27 (br s); 41.95 (br s); 120.13 (br s). IR (cm^{-1}): 1800 (s); 1343 (m); 1226 (s); 1207 (s); 1171 (w); 1095 (m); 1034 (m); 984 (w); 930 (w); 882 (m); 848 (s); 810 (w); 788 (m); 754 (m); 726 (m); 674 (w); 653 (w); 608 (w); 532 (w); 484 (w); 459 (w). Anal. Calcd $C_{22}H_{52}CoN_2P_2Si$. C: 53.52; H: 10.64; N: 5.68. Observed. C: 53.57; H: 10.80; N: 5.78. mp = 135−136 °C. μ_{eff} = 2.0 μ_B.

[N_2P_2]Co (6). A suspension of KC_8 (0.460 g, 3.39 mmol) in 15 mL of THF was added to a solution of **2** (2.00 g, 3.23 mmol) in 15 mL of THF at −40 °C. A color change of green to blue was observed as the reaction mixture warmed to room temperature. Following stirring for 3 h, the volatile materials were removed under vacuum, and the product was extracted with Et_2O (40 mL). The resulting blue solution was passed through a bed of Celite before being concentrated. Cooling at −40 °C overnight resulted in the formation of large dark blue needles in 84% yield (1.34 g). ^{1}H NMR (C_6D_6): δ −30.61 (br s); −0.72 (br s); 0.35 (s); 2.10 (s); 5.75 (s); 10.62 (br s); 12.12 (br s); 18.01 (br s); 31.38 (br s); 35.33 (br s); 42.02 (br s). IR (cm^{-1}): 1345 (s); 1321 (w); 1225 (s); 1170 (m); 1093 (s); 1036 (s); 986 (w); 968 (w); 923 (w); 884 (s); 845 (s); 818 (m); 787 (m); 753 (s); 733 (s); 664 (m); 594 (s); 536 (w); 511 (w); 475 (w); 455 (w). Anal. Calcd for $C_{22}H_{51}CoN_2P_2Si$. C: 53.71; H: 10.47; N: 5.70. Observed. C: 53.96; H: 10.37; N: 5.80. mp = 126−128 °C. μ_{eff} = 3.0 μ_B.

[N_2P_2]Co(CO) (7). Three freeze pump thaw cycles were done on a solution of **6** (0.20 g, 0.41 mmol) in 5 mL of pentane before the addition of 1 equiv of CO. The bright blue solution turned dark green over the course of 1 h, and the reaction mixture was allowed to stir for 2 h. Following concentration and cooling at −40 °C, dark green needles of **7** were isolated in 54% yield (0.13 g). ^{1}H NMR (300 MHz, C_6D_6): δ −30.91 (br s); −9.28 (br s); −2.10 (br s); −0.74 (br s); 0.23 (s); 1.08 (s); 1.81 (s); 2.08 (s); 3.24 (s); 5.67 (br s); 7.80 (br s); 10.40 (br s); 12.09 (br s); 17.99 (br s); 23.08 (br s); 28.46 (br s); 36.48 (br s); 47.30 (br s); 88.47 (br s); 111.37 (br s). IR (cm^{-1}): 1881 (s); 1345 (m); 1305 (w); 1238 (m); 1195 (m); 1115 (w); 1095 (w); 1051 (m); 1017 (w); 969 (w); 926 (w); 908 (w); 882 (w); 840 (s); 793 (m); 753 (m); 731 (m); 678 (w); 652 (m); 605 (m); 530 (w); 464 (w). Anal. Calcd $C_{23}H_{51}CoN_2OP_2Si$. C: 53.05; H: 9.89; N: 5.38. Observed. C: 52.74; H: 9.83; N: 5.13. mp = 151−152 °C. μ_{eff} = 3.0 μ_B.

[^{t}BuN(C=O)SiMe$_2$N(CH$_2$CH$_2$P^{i}Pr$_2$)$_2$]Co(CO)$_2$ (8). Method A. A solution of phenylazide (0.036 g, 0.30 mmol) in 5 mL of pentane was added to a cooled (−116 °C) solution of **6** (0.15 g, 0.30 mmol) in 5 mL of pentane, and a green precipitate formed instantly. The flask was filled with an atmosphere of CO and sealed using a Teflon stopcock. The reaction mixture was allowed to warm to room temperature, during which time the green color faded to yellow. The volatile materials were vacuum transferred for analysis by GCMS. The remaining solid was extracted with toluene, and the resulting solution was stored at −40 °C overnight. Yellow crystals of **8** were collected in 78% yield (0.13 g).

Method B. An atmosphere of CO was introduced to a flask containing a solution of **6** (0.20 g, 0.41 mmol) in 10 mL of pentane at −70 °C. The flask was sealed off, and the reaction mixture was allowed to warm to room temperature and was stirred for 1 h. As the reaction warmed, a yellow precipitate formed. Following the removal of solvent under vacuum, the crude product was extracted with toluene. The yellow solution was concentrated and cooled overnight at −40 °C, resulting in the formation of large yellow crystals in 80% yield (0.19 g).^{1}H NMR (C_6D_6): δ 0.28 (s, 3 H, $SiMe_2$); 0.53 (s, 3 H, $SiMe_2$); 0.86−1.25 (m, 26 H, PCH(C*H*$_3$)$_2$, PC*H*(CH$_3$)$_2$); 1.55 (s, 9 H, ^{t}Bu); 1.67−1.74 (m, 4 H, -CH$_2$CH$_2$-, PC*H*(CH$_3$)$_2$); 1.96 (m, 1 H, -CH$_2$CH$_2$-); 2.30−2.48 (m, 3 H, -CH$_2$CH$_2$-); 2.68−2.76 (m, 2 H, -CH$_2$CH$_2$-).^{13}C NMR (C_6D_6): δ 3.33; 18.00; 18.38; 18.53; 18.77; 19.44; 20.05; 20.65; 22.54; 22.79; 24.09; 24.54; 25.55; 53.70; 56.71; 59.19; 197.98. ^{31}P NMR (C_6D_6): δ 5.80 (s, 1 P); 77.26 (s, 1 P). IR (cm^{-1}): 1952 (s); 1893 (s); 1583 (s); 1359 (m); 1289 (w); 1251 (m); 1197 (m); 1095 (s); 1069 (s); 1033 (m); 990 (m); 924 (w); 884 (w); 840 (w); 824 (w); 804 (w); 778 (w); 726 (w). mp (dec) = 115−117 °C. Anal. Calcd for $C_{25}H_{51}CoN_2O_3P_2Si$. C: 52.06; H, 8.93; N, 4.86. Observed. C: 51.85; H, 9.01; N: 4.75.

[N_2P_2]CoBr (9). Bromine (32 μL, 0.61 mmol) was added via syringe to a solution of **6** (0.30 g, 0.61 mmol) in 10 mL of Et_2O at −40 °C. A green precipitate formed as the reaction mixture warmed to room temperature, and the reaction mixture was stirred for 1 h before the solvent was removed under vacuum. The crude product was extracted with toluene, and following concentration and cooling at −40 °C green crystals of **9** were isolated in 53% yield (0.20 g). ^{1}H NMR (300 MHz, C_6D_6): δ −1.83 (br s); 1.41 (m); 5.55 (br s); 12.85 (br s); 14.24 (br s); 17.47 (br s); 23.65 (br s). IR (cm^{-1}): 1410 (w); 1348 (m); 1307 (w); 1242 (s); 1200 (s); 1106 (m); 1055 (s); 1018 (m); 970 (w); 928 (w); 885 (w); 846 (s); 796 (m); 757 (m); 737 (m); 690 (w); 655 (m); 602 (w); 531 (w); 478 (w). Anal. Calcd C: 46.14; H: 8.99; N: 4.89. Observed. C: 46.03; H: 9.06; N: 4.77. mp = 199−200 °C. μ_{eff} = 4.1 μ_B.

Reaction of 6 with MeI. Methyl iodide (0.087 g, 0.61 mmol) was added to a solution of **6** (0.30 g, 0.61 mmol) in 10 mL of Et_2O at −40 °C. The solution changed color from blue to green and material precipitated. The reaction mixture was allowed to stir for 30 min. Solvent was removed under vacuum, and the crude product was extracted with toluene. Following concentration and cooling at −40°, **2** was isolated in 58% yield (0.24 g).

Reaction of 6 with I_2. A solution of I_2 (0.053 g, 0.21 mmol) in 5 mL of Et_2O was added to a solution of **6** (0.20 g, 0.41 mmol) in 5 mL of Et_2O at −40 °C. The reaction mixture was allowed to

warm to room temperature and was stirred for 1 h over which time the solution changed color from blue to green. Solvent was removed under vacuum, and the crude product was extracted with toluene. Following concentration and cooling at −40 °C, **2** was isolated in 61% yield (0.16 g).

Reaction of 4 with H_2. An atmosphere of H_2 was introduced to a bomb containing a solution of **4** (0.30 g, 0.52 mmol) in 10 mL of THF at room temperature. The reaction mixture was stirred for 2 d. The contents were transferred to a Schlenk tube, and the solvent was removed under vacuum. The crude product was extracted with pentane, and following concentration and cooling **5** was isolated in 73% yield (0.19 g).

$[N_2P_2]CoNHC_6H_5$ (10). Method A. A solution of $LiNHC_6H_5$ (0.048 g, 0.48 mmol) in 5 mL of THF was added to a flask containing a solution of **2** (0.30 g, 0.48 mmol) in 5 mL of THF at −40 °C. The solution color changed from green to red instantly, and the reaction mixture was allowed to warm to room temperature and was stirred overnight. The volatile materials were removed under vacuum, and the crude product was extracted with pentane. The filtrate was concentrated, then stored at −40 °C overnight, resulting in the formation of red-orange blade-like crystals in 72% yield (0.20 g).

Method B. A solution of phenylazide (0.061 g, 0.51 mmol) in 5 mL of pentane was added to a solution of **6** (0.25 g, 0.51 mmol) in 5 mL of pentane at −40 °C, resulting in a color change of blue to dark red concomitant with bubbling. The reaction mixture was allowed to warm to room temperature and was stirred for 2 h. The solution was filtered and concentrated until crystals began to precipitate. The solution was stored at −40 °C overnight, resulting in the formation of red-orange crystals (170 mg, 57%). Repeating the above in THF yielded 102 mg (34%), in toluene 70 mg (23%). ^{1}H NMR (C_6D_6): δ −87.12 (s); −3.20 (br s); −0.82 (s); 0.25 (s); 1.09 (s); 1.18 (s); 1.49 (s); 1.66 (s); 3.25 (s); 4.14 (s); 30.04 (br s); 39.39 (br s). IR (cm^{-1}): 1585 (s); 1486 (m); 1352 (w); 1295 (s); 1243 (m); 1218 (m); 1169 (w); 1073 (m); 1054 (w); 1023 (w); 986 (w); 900 (m); 848 (s); 816 (w); 796 (w); 767 (m); 745 (s); 688 (m); 661 (w); 568 (w); 506 (w). Anal. Calcd for $C_{28}H_{57}CoN_3P_2Si$. C: 57.5; H: 9.84; N: 7.19. Observed. C: 57.28; H: 10.06; N: 7.13. mp = 99−101 °C. μ_{eff} = 3.8 μ_B.

$[N_2P_2]CoNHC_6H_5CH_3$ (11). Method A. The addition of a solution of $LiNHC_6H_5CH_3$ (0.073 g, 0.48 mmol) in 5 mL of THF to a solution of **2** (0.30 g, 0.48 mmol) in 5 mL of THF at −40 °C was accompanied by a color change of dark green to dark red. The reaction mixture was allowed to warm to room temperature and was stirred overnight. Following the removal of the volatile materials under vacuum, the crude product was extracted with pentane, concentrated, and cooled at −40 °C overnight, resulting in the formation of dark red blade-like crystals (0.21 g, 0.35 mmol) in 73% yield.

Method B. A 5 mL solution of *p*-tolylazide (0.068 g, 0.51 mmol) in pentane was added to a solution of **6** (0.25 g, 0.51 mmol) in 5 mL of pentane at −40 °C. The solution changed from blue to dark red instantly upon addition of azide. The reaction mixture was allowed to warm to room temperature and was stirred for 2 h. The solution was filtered and concentrated until crystals began to precipitate. The solution was stored at −40 °C overnight, resulting in the formation of dark red crystals in 32% yield (0.095 g). ^{1}H NMR (C_6D_6): δ −113.03 (br s); −3.09 (s); 0.25 (s); 1.10 (s); 1.67 (s); 3.24 (s); 29.61 (br s); 42.19 (s); 102.05 (s). IR (cm^{-1}): 1605 (s); 1501 (s); 1347 (m); 1289 (s); 1246 (s); 1223 (s); 1173 (m); 1071 (s); 1052 (m); 1036 (m); 933 (w); 899 (m); 846 (s); 809 (s); 771 (s); 758 (m); 741 (s); 691 (w); 666 (w); 608 (w); 579 (w); 546 (m); 505 (m). Anal. Calcd for $C_{29}H_{59}CoN_3P_2Si$. C: 58.23; H: 9.96; N: 7.03. Observed. C: 57.91; H: 9.86; N: 6.72. mp = 105−107 °C. μ_{eff} = 4.1 μ_B.

$[PhN{=}P^iPr_2(CH_2)_2NPh][^tBuNHSiMe_2N(CH_2)_2P^iPr_2]Co$ (12). The compound was isolated by fractional crystallization from the reaction mixture of **10**. Solvent = pentane (<1%); THF (0.025 g, 7.3%); toluene (0.050 g, 15%). ^{1}H NMR (C_6D_6): δ −59.05 (s); −28.92 (s); −25.95 (s); −16.04 (s); −15.49 (s); −6.76 (d); −5.29 (s); −0.76 (s); 0.88 (s); 1.40 (s); 10.23 (s); 15.06 (s); 19.33 (s); 41.91 (s); 49.38 (s); 54.74 (s). IR (cm^{-1}): 3386 (w); 1586 (s); 1301 (m); 1279 (m); 1241 (s); 1179 (m); 1069 (s); 1033 (m); 1005 (s); 984 (m); 922 (w); 903 (s); 837 (m); 815 (m); 778 (m); 741 (m); 700 (m); 663 (w); 621 (w); 601 (w); 526 (w); 494 (w); 466 (w). Anal. Calcd for $C_{34}H_{62}CoN_4P_2Si$. C: 60.41; H: 9.26; N: 8.29. Observed. C: 60.34; H: 8.94; N: 8.57. mp = 132−135 °C. μ_{eff} = 4.1 μ_B.

$ClSiMe_2N(CH_2CH_2P^iPr_2)_2$ (13). A 20 mL pentane solution of Li[PNP] (5.05 g, 16.2 mmol) was added to a solution of Me_2SiCl_2 (2.49 g, 19.3 mmol) in 30 mL of pentane at −40 °C The reaction mixture was warmed to room temperature and was stirred overnight. The solution was filtered, and the remaining white solid was washed with pentane (20 mL). The volatile material was removed under vacuum, leaving **13** in quantitative yield as determined by ^{1}H NMR spectroscopy. Compound **13** was used without further purification. ^{1}H NMR (300 MHz, C_6D_6): δ 0.44 (s, 6 H, $SiMe_2$); 1.03 (m, 24 H, $PCH(CH_3)_2$); 1.62 (m, 8 H, $PCH(CH_3)_2$ and $-CH_2CH_2-$); 3.18 (m, 4 H, $-CH_2CH_2-$). ^{31}P NMR (400 MHz, C_6D_6): δ 1.10 (s).

$H[N_2P_2^{tolyl}]$ (14). A solution of **13** (6.45 g, 16.2 mmol) in 20 mL of pentane was added dropwise to a suspension of $LiNHC_6H_4CH_3$ (1.83 g, 16.2 mmol) in 30 mL of pentane at −40 °C. The reaction mixture was allowed to warm to room temperature and was stirred overnight. The solution was filtered, and the remaining solid was washed with pentane (30 mL). Solvent was removed under vacuum leaving **14** as an orange oil in 90% yield (6.83 g). ^{1}H NMR (300 MHz, C_6D_6): δ 0.26 (s, 6 H, $SiMe_2$); 1.10 (m, 24 H, $PCH(CH_3)_2$); 1.56 (m, 8 H, $PCH(CH_3)_2$ and $-CH_2CH_2-$); 2.17 (s, 3 H, Ar-CH_3); 3.22 (m, 4 H, $-CH_2CH_2-$); 6.68 (d, 2 H, J_{HH} = 8 Hz, Ar−H); 6.97 (d, 2 H, J_{HH} = 8 Hz, Ar−H). ^{31}P NMR (400 MHz, C_6D_6): δ −1.66 (s).

$Li[N_2P_2^{tolyl}]$ (15). *N*-butyl lithium (1.6 M in hexanes, 10 mL, 16 mmol) was syringed to a solution of **14** (7.5 g, 16 mmol) in 40 mL of pentane at −70 °C. The reaction mixture was warmed to room temperature and was stirred for 3 h. The reaction flask was cooled at −40 °C, resulting in the formation and isolation of colorless crystals in 71% yield (5.4 g). ^{1}H NMR (300 MHz, C_6D_6): δ 0.58 (s, 6 H, $SiMe_2$); 0.97 (m, 24 H, $PCH(CH_3)_2$); 1.41 (m, 4 H, $PCH(CH_3)_2$); 1.59 (m, 4 H, $-CH_2CH_2-$); 2.29 (s, 3 H, Ar-CH_3); 3.03 (m, 4 H, $-CH_2CH_2-$); 6.93 (d, 2 H, J_{HH} = 8.4 Hz, Ar−H); 7.05 (d, 2 H, J_{HH} = 8.4 Hz, Ar−H); ^{31}P NMR (400 MHz, C_6D_6): δ −3.35 (br s). IR (cm^{-1}): 1603 (m); 1377 (m); 1286 (s); 1247 (m); 1172 (w); 1088 (m); 1056 (m); 992 (w); 951 (s); 899 (m); 822 (s); 765 (m); 718 (w); 699 (w); 667 (w); 650 (w); 605 (w); 510 (m). Anal. Calcd $C_{25}H_{49}LiN_2P_2Si$. C: 63.25; H: 10.42; N: 5.90. Observed. C: 63.08; H: 10.45; N: 5.68. mp = 133−134 °C.

$[N_2P_2^{tolyl}]CoI$ (16). A solution of **15** (2.0 g, 4.2 mmol) was added dropwise to a suspension of CoI_2 (1.3 g, 4.2 mmol) in 20 mL of toluene, and the reaction mixture was stirred overnight. Solvent was removed under vacuum, and the crude product was dissolved in THF and filtered through a bed of Celite. An equal volume of pentane was added, and the resulting solution was cooled at −40 °C overnight. Brown crystals were isolated in 80% yield (2.2 g). ^{1}H NMR (500 MHz, C_6D_6): δ −53.11 (br s); 0.96 (m); 8.99 (s); 10.72 (s); 12.40 (s); 22.24 (s); 39.16 (s); 52.96 (br s); 55.21 (s); 66.75 (br s); 67.97 (br s); 92.70 (br s). IR (cm^{-1}): 1604 (s); 1500

Table 2. Crystal Data and Structure Refinement for **2**−**8**, **10**, **12**, **16**, and **17**

compound number	**2**	**3**	**4**	**5**	**6**	**7**
compound name	$[N_2P_2]$CoI	$[N_2P_2]$CoMe	$[N_2P_2]CoCH_2SiMe_3$	$[N_2P_2]$CoH	$[N_2P_2]$Co	$[N_2P_2]$Co(CO)
empirical formula	$C_{22}H_{51}CoIN_2P_2Si$	$C_{23}H_{54}CoN_2P_2Si$	$C_{26}H_{62}CoN_2P_2Si_2$	$C_{22}H_{52}CoN_2P_2Si$	$C_{22}H_{51}CoN_2P_2Si$	$C_{23}H_{51}CoN_2OP_2Si$
fw	619.51	507.64	579.83	493.62	492.61	520.62
temperature (K)	168(2)	114(2)	158(2)	168(2)	244(2)	168(2)
crystal system	monoclinic	monoclinic	triclinic	orthorhombic	orthorhombic	orthorhombic
space group	$P2_1/c$	$P2_1/c$	$P\bar{1}$	$Pna2_1$	$Pnma$	$P2_12_12_1$
a (Å)	9.356(2)	16.546(6)	8.6829(5)	15.0594(19)	14.742(4)	11.409(4)
b (Å)	34.812(8)	11.679(4)	9.8323(6)	10.9722(14)	11.265(3)	15.440(5)
c (Å)	9.299(2)	14.610(5)	21.6331(12)	16.739(2)	17.148(5)	16.068(6)
α (deg)	90	90	98.3500(10)	90	90	90
β (deg)	105.015(4)	91.834(5)	99.4850(10)	90	90	90
γ (deg)	90	90	103.8940(10)	90	90	90
V (Å^3)	2925.4(11)	2821.8(18)	1735.09(17)	2765.8(6)	2847.6(13)	2830.5(17)
Z	4	4	2	4	4	4
λ (Å)	0.71073	0.71073	0.71073	0.71073	0.71073	0.71073
μ (cm^{-1})	1.804	0.776	0.672	0.79	0.768	0.778
no. of refl	5914	2772	5916	3695	2931	3509
R(int)	0.0457	0.1043	0.0258	0.0257	0.0423	0.0989
R_{obs} (%)	3.96	5.67	4.03	2.84	5.28	6.32
R_{wobs} (%)	8.81	12.28	12.22	7.23	14.29	14.59

compound number	**8**	**10**	**12**	**16**	**17**
compound name	[^{t}BuN(C═O)SiMe$_2$N-(CH$_2$CH$_2$P^{i}Pr$_2$)$_2$]Co(CO)$_2$	$[N_2P_2]$CoNHC$_6$H$_5$	[PhN═P^{i}Pr$_2$(CH$_2$)$_2$NPh]-[^{t}BuNHSiMe$_2$N(CH$_2$)$_2$P^{i}Pr$_2$]Co	$[N_2P_2^{tolyl}]$CoI	$[N_2P_2^{tolyl}]$Co
empirical formula	$C_{25}H_{51}CoN_2O_3P_2Si$	$C_{28}H_{57}CoN_3P_2Si$	$C_{34}H_{62}CoN_4P_2Si$	$C_{25}H_{49}CoIN_2P_2Si$	$C_{25}H_{49}CoN_2P_2Si$
fw	576.64	584.73	675.84	653.52	526.62
temperature (K)	160(2)	151(2)	167(2)	151(2)	124(2)
crystal system	monoclinic	monoclinic	monoclinic	monoclinic	monoclinic
space group	$P2_1$	$P2_1/n$	$P2_1/n$	$P2_1/c$	$P2_1/c$
a (Å)	8.3023(11)	13.154(5)	11.044(3)	12.2546(14)	13.176(2)
b (Å)	12.2795(17)	15.801(6)	14.324(4)	13.8526(16)	14.784(3)
c (Å)	15.354(2)	16.304(6)	23.454(6)	17.881(2)	14.826(3)
α (deg)	90	90	90	90	90
β (deg)	93.718(2)	102.657(5)	93.105(4)	101.541(2)	91.062(2)
γ (deg)	90	90	90	90	90
V (Å^3)	1562.1(4)	3307(2)	3704.7(16)	2974.0(6)	2887.5(9)
Z	2	4	4	4	4
λ (Å)	0.71073	71073	0.71073	0.71073	0.71073
μ (cm^{-1})	0.716	0.672	0.61	1.779	0.762
no. of refl	5638	4423	7547	3642	4328
R(int)	0.0336	0.0745	0.0455	0.0774	0.0247
R_{obs} (%)	4.17	5.31	4.36	4.24	4.46

(s); 1303 (w); 1256 (s); 1242 (m); 1181 (w); 1167 (w); 1106 (s); 1062 (m); 1044 (m); 997 (w); 970 (w); 920 (s); 883 (w); 842 (s); 819 (m); 795 (m); 770 (s); 684 (m); 661 (m); 620 (w); 597 (w); 548 (w); 514 (m); 481 (w). Anal. Calcd $C_{25}H_{49}CoIN_2P_2Si$. C: 45.94; H: 7.57; N: 4.29. Observed. C: 45.97; H: 7.61; N: 4.24. mp = 208−209 °C. μ_{eff} = 4.2 μ_B.

[N$_2$P$_2^{tolyl}$]Co (17). A suspension of KC_8 (0.42 g, 3.1 mmol) in 10 mL of DME was added to a brown solution of **16** (2.0 g, 3.0 mmol) in 15 mL of DME at −40 °C. A color change from brown to green was observed as the reaction mixture warmed to room temperature. Following stirring for 3 h, the solvent was removed under vacuum, and the crude product was extracted with pentane. The green solution was concentrated and cooled at −40 °C overnight, resulting in the isolation of green crystals in 72% yield (1.2 g). ^{1}H NMR (500 MHz, C_6D_6): δ −66.52 (br s); −30.26 (br s); −0.33 (s); 0.88 (s); 3.49 (s); 8.25 (br s); 12.38 (br s); 15.59 (br s); 26.15 (s); 32.38 (br s); 39.84 (br s); 41.64 (br s); 65.57 (s); 106.75 (br s). IR (cm^{-1}): 1602 (m); 1377 (m); 1317 (s); 1244 (m); 1172 (w); 1088 (w); 1039 (m); 959 (m); 908 (w); 883 (w); 831 (m); 813 (m); 762 (w); 739 (w); 666 (m); 634 (w); 605 (m); 553 (w); 516 (w); 460 (w). Anal. Calcd $C_{25}H_{49}CoN_2P_2Si$. C: 57.00; H: 9.40; N: 5.32. Observed. C: 56.91; H: 9.48; N: 5.31. mp = 85−87 °C. μ_{eff} = 3.0 μ_B.

[N$_2$P$_2^{tolyl}$]Co(CO) (18). Three freeze pump thaw cycles were done on a solution of **17** (0.20 g, 0.38 mmol) in 5 mL of Et$_2$O before 1 equiv of CO was added. The green solution turned slightly yellow and material precipitated. The reaction mixture was stirred for 2 h. Solvent was removed under vacuum, and the crude product was extracted with toluene. Following concentration and cooling at −40 °C, dark red blocks of **18** were isolated in 43% yield (0.090 g). ^{1}H NMR (300 MHz, C_6D_6): δ −1.83 (br s); 0.27 (s); 1.07 (s); 1.32 (s); 1.58 (s); 1.82 (s); 2.16 (s); 6.07 (br s); 12.31 (br s); 15.53 (br s); 20.04 (br s); 27.49 (br s); 42.49 (br s); 65.22 (br s). IR (cm^{-1}): 1898 (s); 1605 (m); 1497 (s); 1314 (m); 1268 (s); 1246 (m); 1179 (w); 1111 (w); 1093 (w); 1045 (w); 928 (m); 885 (w); 839 (m); 817 (m); 801 (m); 757 (m); 672 (w); 600 (w); 516 (w); 458 (w). Anal. Calcd $C_{26}H_{49}CoN_2OP_2Si$. C: 56.29; H: 8.92; N: 5.05. Observed. C: 56.34; H: 9.24; N: 4.87. mp = 162−163 °C. μ_{eff} = 2.8 μ_B.

Crystallographic Analysis. Single crystals of **2**−**8**, **10**, **12**, **16**, and **17** were coated in Paratone-N oil, mounted on a Kaptan loop, transferred to a Siemens SMART diffractometer or a Bruker APEX CCD area detector,[34] centered in the beam, and cooled by a nitrogen flow low-temperature apparatus that has been previously calibrated by a thermocouple placed at the same position as the crystal. Preliminary orientation matrices and cell constants were determined by collection of 60 30-s frames, followed by spot integration and least-squares refinement. An arbitrary hemisphere of data was collected, and the raw data were integrated using SAINT.[35] Cell dimensions reported were calculated from all reflections with $I >$

(34) *SMART Area-Detector Software Package*; Bruker Analytical X-ray Systems, Inc.: Madison, WI, 1995−1999.
(35) *SAINT SAX Area-Detector Integration Program*, V7.06; Siemens Industrial Automation, Inc.: Madison, WI, 2005.

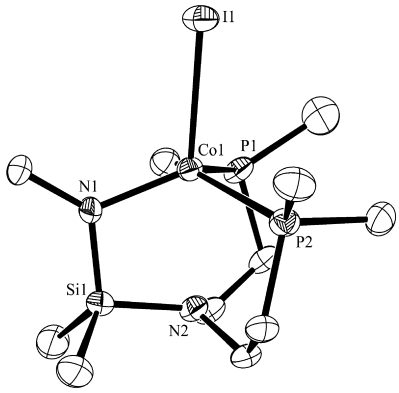

Figure 1. Thermal ellipsoid (50%) plot of **2**. Hydrogen atoms, *iso*-propyl methyl, and *tert*-butyl methyl groups have been omitted for clarity.

10σ. The data were corrected for Lorentz and polarization effects, but no correction for crystal decay was applied. Data were analyzed for agreement and possible absorption using XPREP.[36] An empirical absorption correction based on comparison of redundant and equivalent reflections was applied using SADABS.[37] The structures were solved using SHELXS[38] and refined on all data by full-matrix least-squares with SHELXL-97.[39] Thermal parameters for all non-hydrogen atoms were refined anisotropically. Oak Ridge Thermal Ellipsoid Plot (ORTEP) diagrams were created using ORTEP-3. A summary of the X-ray diffraction data is presented in Table 2.

Results and Discussion

As an entry into Co(II) organometallic and reduced metal species, the synthesis of metal-halide starting materials $[N_2P_2]$CoX (X = Cl, I) was explored. The synthesis of $[N_2P_2]$CoCl (**1**) has been described previously,[28] and $[N_2P_2]$CoI (**2**) was synthesized through an analogous reaction to that of **1** but with toluene as the reaction solvent. Dark green blocks of **2** were isolated in 83% yield following crystallization from toluene at −40 °C. The solution magnetic susceptibilities of **1** and **2** (4.1 μ_B and 4.0 μ_B, respectively) agree with an $S = {}^3/_2$ spin-state (high-spin). The solid-state structures of **1** and **2** display similar structural features with both Co(II) centers lying in distorted tetrahedral geometries (Figure 1). Relevant bond lengths and angles are provided in Table 3. The significantly higher isolated yield of **2** compared to that of **1** distinguished it as the starting material of choice.

Substitution Chemistry of 2. Supporting ligands used for the stabilization of reactive metal fragments are often susceptible to undesirable, non-innocent behavior. In the case of organometallic complexes, for example, the polarity of M−C bonds renders them especially reactive and for TDMA systems, decomposition of the supporting ligand via intramolecular C−H bond activation has been observed. To probe the stability of the $[N_2P_2]$ ligand under these circumstances, the synthesis of various organometallic complexes was attempted.

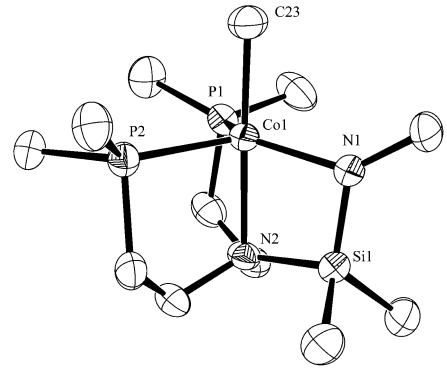

Figure 2. Thermal ellipsoid (50%) plot of **3**. Hydrogen atoms, *iso*-propyl methyl, and *tert*-butyl methyl groups have been omitted for clarity.

Table 3. Selected Bond Lengths (Å) and Angles (deg) for $[N_2P_2]$CoI (**2**)

Co(1)−I(1)	2.7229(7)	Co(1)−P(1)	2.3947(12)
Co(1)−N(1)	1.957(3)	Co(1)−P(2)	2.3993(13)
N(1)−Co(1)−P(1)	119.01(10)	N(1)−Co(1)−P(2)	112.20(10)
P(1)−Co(1)−P(2)	107.43(4)	N(1)−Co(1)−I(1)	114.58(9)
P(1)−Co(1)−I(1)	96.55(3)	P(2)−Co(1)−I(1)	105.30(4)

Scheme 1. Synthesis of $[N_2P_2]$CoR Complexes

$[N_2P_2]$CoI + LiR $\xrightarrow[\text{LiCl}]{\text{Et}_2\text{O (a), THF (b)}}$ $[N_2P_2]$CoR

a: R = -CH_3 (**3**)

b: R = -CH_2SiMe_3 (**4**)

Table 4. Selected Bond Lengths (Å) and Angles (deg) for $[N_2P_2]$CoMe (**3**)

Co(1)−N(1)	1.985(4)	Co(1)−C(23)	1.995(5)
Co(1)−N(2)	2.134(4)	Co(1)−P(2)	2.2636(15)
Co(1)−P(1)	2.2647(16)		
N(1)−Co(1)−C(23)	98.96(18)	N(1)−Co(1)−N(2)	78.48(14)
C(23)−Co(1)−N(2)	177.23(19)	N(1)−Co(1)−P(2)	124.15(13)
C(23)−Co(1)−P(2)	94.67(16)	N(2)−Co(1)−P(2)	85.97(11)
N(1)−Co(1)−P(1)	124.03(13)	C(23)−Co(1)−P(1)	95.72(16)
N(2)−Co(1)−P(1)	86.65(11)	P(2)−Co(1)−P(1)	107.87(6)

Reaction of **2** with MeLi (1.6 M in Et_2O) in Et_2O resulted in the isolation of $[N_2P_2]$CoMe (**3**) as dark green crystals in 53% yield following crystallization from pentane at −40 °C (Scheme 1a). Crystals suitable for an X-ray diffraction study were grown from an Et_2O solution at −40 °C, and an ORTEP diagram is shown in Figure 2 with selected bond lengths and angles provided in Table 4. The geometry of **3** has altered from distorted tetrahedral in **2** to trigonal bipyramidal by a change in the binding mode of the $[N_2P_2]$ ligand from κ^3-NP_2 to κ^4-N_2P_2. A change in the spin-state is also observed with the solution magnetic susceptibility of **3** indicating the presence of a low-spin species (μ_{eff} = 1.8 μ_B). The Co(1)−C(23) bond distance of 1.994(5) Å is slightly shorter than the values observed in the related Co(II) compounds $[Ph_2PC_6H_4N(H)]CoMe(PMe_3)_2$ (2.019(3) Å, C.N. = 5),[40] [PhTt^{tBu}]CoMe (2.052(3) Å, C.N. = 4),[41] PhB(^{t}BuIm)$_3$CoMe (2.042(2) Å, C.N. = 4),[42] and [Tp$^{t\text{-Bu,Me}}$]CoMe (2.115(14)

(36) *XPREP, Part of the SHELXTL Crystal Structure Determination Package*, v6.12; Bruker AXS Inc.: Madison, WI, 1995.
(37) Sheldrick, G. *SADABS, Siemens Area Detector ABSorption correction program*, v2.10; Siemens Industrial Automation, Inc.: Madison, WI, 2005.
(38) *XS Program for the Refinement of X-ray Crystal Structures, Part of the SHELXTL Crystal Structure Determination Package*; Bruker Analytical X-ray Systems, Inc.: Madison, WI, 1995−1999.
(39) *XL Program for the Refinement of X-ray Crystal Structures, Part of the SHELXT Crystal Structure Determination Package*; Bruker Analytical X-ray Systems, Inc.: Madison, WI, 1995−1999.
(40) Klein, H. F.; Beck, R.; Florke, U.; Haupt, H. J. *Eur. J. Inorg. Chem.* **2003**, 240–248.

Table 5. Selected Bond Lengths (Å) and Angles (deg) for $[N_2P_2]CoCH_2SiMe_3$ (**4**)

Co(1)−N(1)	1.9261(18)	Co(1)−C(23)	2.033(2)
Co(1)−N(2)	2.2499(17)	Co(1)−P(1)	2.4089(6)
N(1)−Co(1)−C(23)	122.93(9)	N(1)−Co(1)−N(2)	76.56(7)
C(23)−Co(1)−N(2)	111.41(8)	N(1)−Co(1)−P(1)	117.71(6)
C(23)−Co(1)−P(1)	119.27(7)	N(2)−Co(1)−P(1)	84.63(5)

Table 6. Selected Bond Lengths (Å) and Angles (deg) for $[N_2P_2]CoH$ (**5**)

Co(1)−N(1)	1.9301(18)	Co(1)−N(2)	2.1069(17)
Co(1)−P(2)	2.1974(9)	Co(1)−P(1)	2.2052(9)
Co(1)−H(52)	1.39(3)		
N(1)−Co(1)−N(2)	80.38(7)	N(1)−Co(1)−P(2)	127.66(10)
N(2)−Co(1)−N(2)	88.78(8)	N(1)−Co(1)−P(1)	116.51(10)
N(2)−Co(1)−N(1)	88.73(8)	N(2)−Co(1)−P(1)	114.22(3)
N(1)−Co(1)−N(52)	99.4(11)	N(2)−Co(1)−P(52)	179.0(18)
N(2)−Co(1)−N(52)	90.6(17)	N(1)−Co(1)−P(52)	92.3(17)

Å, C.N. = 4).[43] The remaining bond distances are also very similar to those observed in $[Ph_2PC_6H_4N(H)]CoMe(PMe_3)_2$ (C.N. = 5).[40]

Reaction of **2** with $LiCH_2SiMe_3$ resulted in the formation of $[N_2P_2]CoCH_2SiMe_3$ (**4**), which was isolated in 57% yield as large lime-green plates following crystallization from pentane at −40 °C (Scheme 1b). The solution magnetic susceptibility of **4** is 4.2 μ_B, indicating a potential difference in the geometry around the Co(II) center compared to that found in **3**. To determine if this were the case, the solid-state structure of **4** was determined via X-ray diffraction (see Figure 3; selected bond lengths and angles are provided in Table 5). In contrast to **1**−**3**, the $[N_2P_2]$ ligand is bound κ^3-N_2P in compound **4**. One phosphine arm in **4** remains uncoordinated likely because of steric congestion at the Co center. The geometry around the Co atom is tetrahedral, and the Co(1)−C(23) bond distance of 2.033(2) Å is very close to the values seen in the two previously reported examples (P−P)CoCl(CH_2SiMe_3) (2.013(2) Å) and (P−P)Co(CH_2SiMe_3)$_2$ (2.039(7) and 2.043(7) Å), where (P−P) is a phosphorus-bridged ferrocenophane ligand.[44]

Late metal hydrides are well-known and have been shown to play key roles in a wide range of stoichiometric and catalytic transformations.[45−49] The reactivity of **3** and **4** with H_2 was explored to determine if either was a useful starting material for a metal-hydride. A flask containing a solution of **3** in THF was heated at 65 °C for 72 h under an atmosphere of H_2, but no reaction was observed. In contrast, exposure of compound **4** to H_2 at 1 atm over 48 h at room

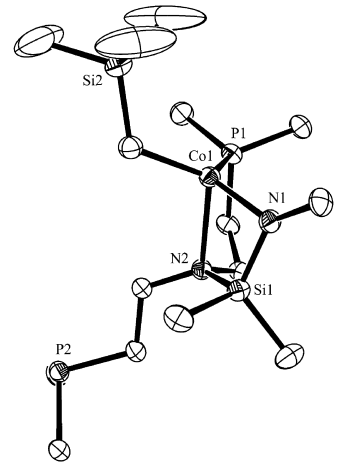

Figure 3. Thermal ellipsoid (50%) plot of **4**. Hydrogen atoms, *iso*-propyl methyl, and *tert*-butyl methyl groups have been omitted for clarity.

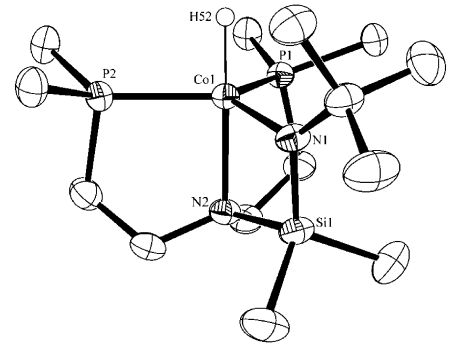

Figure 4. Thermal ellipsoid (50%) plot of **5**. Hydrogen atoms, and *iso*-propyl methyl groups have been omitted for clarity.

temperature resulted in the clean formation of $[N_2P_2]CoH$ (**5**), which was isolated as dark olive needles in 73% yield. The IR spectrum of **5** features a sharp absorption at 1800 cm^{-1}, indicative of a metal-hydride moiety. The solution magnetic susceptibility of **5** is 2.0 μ_B ($S = {}^1/_2$), similar to that in **3**. An X-ray diffraction study confirmed the geometry around the Co atom as trigonal bipyramidal. An ORTEP diagram is shown in Figure 4 with selected bond lengths and angles provided in Table 6. As in compound **3**, the ligand in **5** is bound κ^4-N_2P_2 with similar metal−ligand geometrical parameters. The hydride was located in the Fourier map and refined to give a Co−H bond distance of 1.39(3) Å, in agreement with other crystallographically characterized Co−H compounds.[50] A number of factors such as coordination number and spin-state may discourage the reactivity of H_2 with **3** compared to that of **4** and H_2. Complex **5** was also synthesized by reaction of **2** with alkylating reagents containing β-hydrogens such as ethyl magnesium chloride and *n*-BuLi (Scheme 2). One likely mechanism for this transformation involves β-hydride elimination by a transient Coalkyl species, which results in the release of alkene and the formation of **5**. We note that in an effort to probe the reverse of this process, no reaction was observed between **5** and 1 atm ethylene in a sealed NMR tube at room temperature.

Reduction Chemistry of 2. Chemical reduction of compound **2** was explored to determine whether a low-valent

(41) Schebler, P. J.; Mandimutsira, B. S.; Riordan, C. G.; Liable-Sands, L. M.; Incarvito, C. D.; Rheingold, A. L. *J. Am. Chem. Soc.* **2001**, *123*, 331–332.
(42) Cowley, R. E.; Bontchev, R. P.; Duesler, E. N.; Smith, J. M. *Inorg. Chem.* **2006**, *45*, 9771–9779.
(43) Jewson, J. D.; Liable-Sands, L. M.; Yap, G. P. A.; Rheingold, A. L.; Theopold, K. H. *Organometallics* **1999**, *18*, 300–305.
(44) Imamura, Y.; Mizuta, T.; Miyoshi, K.; Yorimitsu, H.; Oshima, K. *Chem. Lett.* **2006**, *35*, 260–261.
(45) Sadique, A. R.; Gregory, E. A.; Brennessel, W. W.; Holland, P. L. *J. Am. Chem. Soc.* **2007**, *129*, 8112–8121.
(46) Yu, Y.; Sadique, A. R.; Smith, J. M.; Dugan, T. R.; Cowley, R. E.; Brennessel, W. W.; Flaschenriem, C. J.; Bill, E.; Cundari, T. R.; Holland, P. L. *J. Am. Chem. Soc.* **2008**, *130*, 6624–6638.
(47) Bart, S. C.; Bowman, A. C.; Lobkovsky, E.; Chirik, P. J. *J. Am. Chem. Soc.* **2007**, *129*, 7212.
(48) Bart, S. C.; Lobkovsky, E.; Chirik, P. J. *J. Am. Chem. Soc.* **2004**, *126*, 13794–13807.
(49) Krische, M. J.; Yongkui, S. *Acc. Chem. Res.* **2007**, *40*, 1237–1237.
(50) Allen, F. H. *Acta Crystallogr.* **2002**, *B58*, 380–388.

Scheme 2. Synthesis of **5**

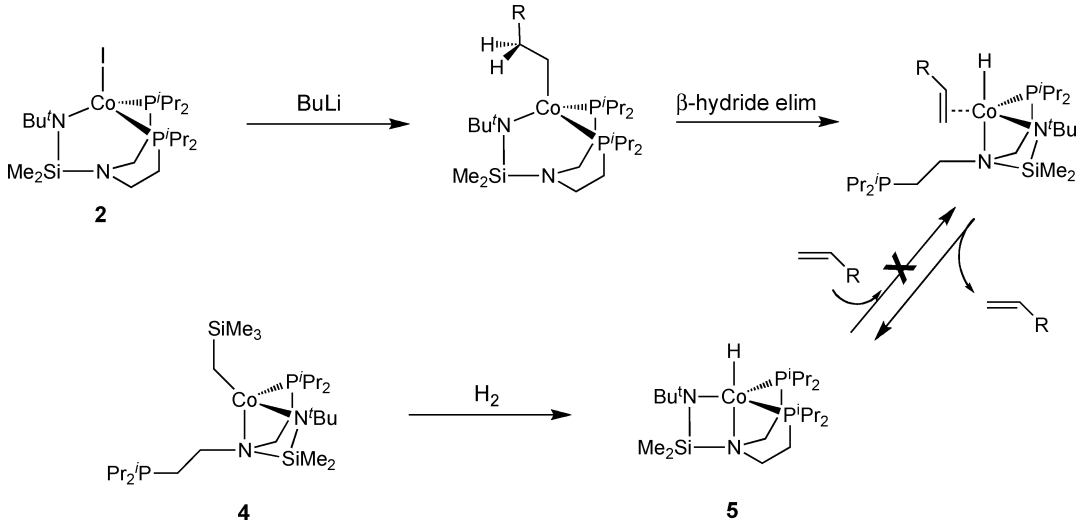

Co species could be isolated. Reduction of **2** with KC_8 in THF resulted in a color change of dark green to deep blue and allowed for the isolation of $[N_2P_2]Co$ (**6**) in 84% yield as large blue needles following crystallization from Et_2O at −40 °C. The results of an X-ray diffraction study of **6** are shown in Figure 5, with selected bond lengths and distances provided in Table 7. An open axial coordination site was created upon reduction and alteration of the coordination mode of the $[N_2P_2]$ ligand from κ^3-NP_2 in **2** to κ^4-N_2P_2 in **6**. The geometry around the Co center is trigonal pyramidal,[10] and the solution magnetic susceptibility of **6** (3.0 μ_B), in accord with an $S = 1$ ground state.

The reactivity of **6** with a number of small molecules including N_2, MeI, I_2, Br_2, H_2, CO, ethylene, $N_3{}^tBu$, H_3SiPh, and N_3Ar (Ar = C_6H_5, $C_6H_4CH_3$) was surveyed. Unlike related Co compounds,[6,51] compound **6** does not coordinate N_2 in solution or the solid-state as demonstrated by IR spectroscopy and X-ray diffraction studies. Exposure of a pentane solution of **6** to 1 equiv of CO resulted in a solution color change of blue to green upon warming to room temperature. Following concentration and cooling of the solution at −40 °C, dark green needles of $[N_2P_2]Co(CO)$ (**7**) were isolated in 54% yield. A single, strong absorption in the IR spectrum at 1881 cm^{-1} supports the formation of a monocarbonyl and is in agreement with similar four coordinate Co(I) carbonyl complexes.[52,53] However, the ν_{CO} is significantly lower than the value observed in $Tp^{Np}Co(CO)$ (1950 cm^{-1})[54] and CpCo(CO) (1993−1999 cm^{-1})[55,56] Further confirmation of the connectivity of **7** was achieved by an X-ray diffraction study (see Figure 6 and Table 8). Coordination by the basal nitrogen is no longer observed in **7**, with the binding mode of the $[N_2P_2]$ ligand returning again to κ^3-NP_2, as was observed in the solid-state structures of **1** and **2**. The solution magnetic susceptibility of **7** (3.0 μ_B) is in agreement with a high-spin Co(I) center.

A quite different carbonyl derivative was obtained when **6** was exposed to an *excess* of CO. Addition of an atmosphere of CO to a solution of **6** in pentane at −70 °C resulted in a color change of blue to yellow with concomitant formation of a precipitate. Following the removal of solvent under vacuum, extraction with toluene, concentration, and cooling

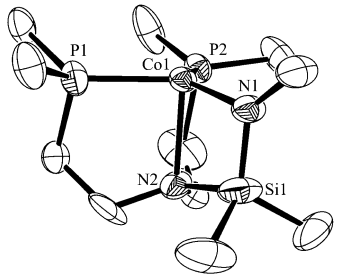

Figure 5. Thermal ellipsoid (50%) plot of **6**. Hydrogen atoms, *iso*-propyl methyl, and *tert*-butyl methyl groups have been omitted for clarity.

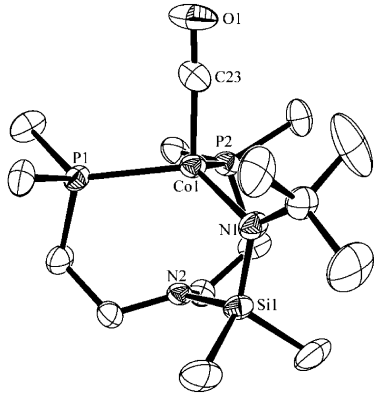

Figure 6. Thermal ellipsoid (50%) plot of **7**. Hydrogen atoms, *iso*-propyl methyl, and *tert*-butyl methyl groups have been omitted for clarity.

Table 7. Selected Bond Lengths (Å) and Angles (deg) for $[N_2P_2]Co$ (**6**)

Co(1)−N(1)	1.917(4)	Co(1)−P(1)	2.2124(11)
Co(1)−N(2)	2.207(4)	Co(1)−P(2)	2.2124(11)
N(1)−Co(1)−P(1)	126.46(4)	N(1)−Co(1)−P(2)	126.46(4)
P(1)−Co(1)−P(2)	105.17(6)	N(1)−Co(1)−N(2)	79.76(18)
P(2)−Co(1)−P(2)	88.91(8)	N(1)−Co(1)−N(2)	88.92(8)

Table 8. Selected Bond Lengths (Å) and Angles (deg) for $[N_2P_2]Co(CO)$ (**7**)

Co(1)−C(23)	1.800(7)	Co(1)−N(1)	1.966(5)
Co(1)−P(2)	2.294(2)	Co(1)−P(1)	2.302(2)
O(1)−C(23)	1.151(8)		
C(23)−Co(1)−N(1)	113.0(3)	C(23)−Co(1)−P(2)	103.0(2)
N(1)−Co(1)−P(2)	112.50(19)	C(23)−Co(1)−P(1)	97.7(2)
N(1)−Co(1)−P(1)	123.20(18)	P(2)−Co(1)−P(1)	104.82(7)

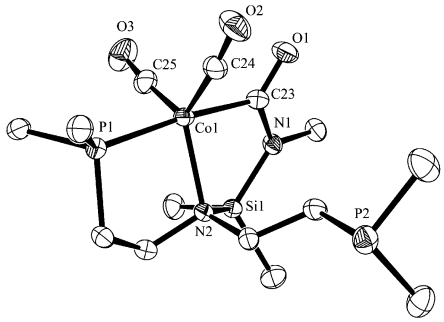

Figure 7. Thermal ellipsoid (50%) plot of **8**. Hydrogen atoms, *iso*-propyl methyl, and *tert*-butyl methyl groups have been omitted for clarity.

Table 9. Selected Bond Lengths (Å) and Angles (deg) for [^{t}BuN(C═O)SiMe$_2$N((CH$_2$)$_2$P^{i}Pr$_2$)$_2$]Co(CO)$_2$ (**8**)

Co(1)−C(23)	1.983(4)	Co(1)−C(24)	1.765(4)
Co(1)−C(25)	1.740(4)	Co(1)−N(2)	2.114(3)
Co(1)−P(1)	2.2379(10)		
C(25)−Co(1)−C(24)	117.5(2)	C(25)−Co(1)−C(23)	86.45(16)
C(24)−Co(1)−C(23)	88.13(15)	C(25)−Co(1)−N(2)	119.16(15)
C(24)−Co(1)−N(2)	122.92(17)	C(23)−Co(1)−N(2)	88.88(13)
C(25)−Co(1)−P(1)	95.78(13)	C(24)−Co(1)−P(1)	95.34(11)
C(23)−Co(1)−P(1)	174.42(11)	N(2)−Co(1)−P(1)	85.57(8)

at −40 °C, yellow crystals of the diamagnetic complex [^{t}BuN(C═O)SiMe$_2$N((CH$_2$)$_2$P^{i}Pr$_2$)$_2$]Co(CO)$_2$ (**8**) were isolated in 80% yield. In contrast to the IR spectrum of **7**, complex **8** shows three C−O bands at 1952, 1893, and 1583 cm^{-1}. An X-ray diffraction study (Figure 7; Table 9) confirmed the connectivity of **8**. The low frequency stretch at 1583 cm^{-1} is assigned to the CO molecule that has inserted itself into the Co−amide bond.[57−59] The Co atom adopts a trigonal bipyramidal geometry with one "dangling" phosphine because of electronic saturation (18 e$^-$) at the metal center. Compound **8** demonstrates the stronger affinity of the Co(I) center to CO over the neutral phosphine, as expected.

The reactivity of **6** with various oxidants was also explored. Reaction of **6** with 1 equiv of MeI in THF resulted in a solution color change of blue to dark green. Following the removal of solvent under vacuum, extraction with toluene, concentration, and cooling at −40 °C, dark green blocks of **2** were isolated in 53% yield. Similar results were obtained from the reaction of **6** with 1 equiv of I_2 (Scheme 3). In contrast to related work by Caulton *et al.,* the formation of a Zwitterionic product by addition of a second equivalent of I_2 was not observed.[60] Reaction of **6** with a stronger

Scheme 3. Oxidation Reactions with **6**

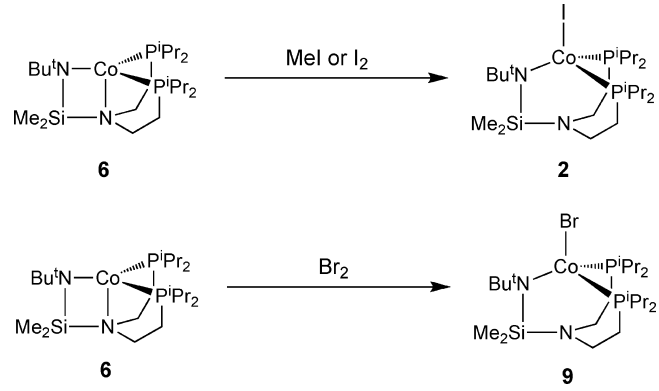

oxidant such as Br_2 was also examined, and again the reaction of **6** with 1 equiv of Br_2 resulted in the exclusive isolation of [N_2P_2]CoBr (**9**) in 53% yield. Similar to **1** and **2**, the solution magnetic susceptibility of **9** is 4.1 μ_B, indicative of a high-spin metal center. The reaction of **6** with H_2 and ethylene was also examined; however, no reaction between these substrates and the Co(I) center was observed.

Generation and Reactivity of Transient Co(III) Imido Species. Initial attempts to synthesize a Co(III) imido species by the addition of N$_3$^{t}Bu to **6** only resulted in the isolation of starting material. In contrast, reaction of phenylazide with **6** in pentane takes place rapidly at −116 °C (Et$_2$O/N$_2$(*l*)) to form a green precipitate (**A**). When allowed to warm to room temperature, species **A** quickly disappeared and a dark red solution was formed. When phenylazide was added to a solution of **6** at or above −70 °C, a similar dark red solution formed immediately. Following filtration, concentration, and cooling, red-orange crystals of [N_2P_2]CoNHPh (**10**) were collected in 57% yield. Analogous results were observed with *p*-tolylazide, and [N_2P_2]CoNHC$_6$H$_4$CH$_3$ (**11**) was isolated in 32% yield as red blocks following crystallization from pentane at −40 °C.

An ORTEP diagram showing the molecular structure of **10** is given in Figure 8, with selected bond lengths and angles provided in Table 10. As was observed in the case of **4**, the [N_2P_2] ligand is bound κ^3-N_2P with one "dangling" phosphine because of steric congestion around the metal center. The geometry about the Co is best described as distorted tetrahedral with angles of 77.03(16)° {N(1)−Co(1)−N(2)}, 118.23(13)°{N(1)−Co(1)−P(1)},131.49(17)°{N(1)−Co(1)−N(3)}, and 109.78(16)° {N(2)−Co(1)−N(3)}. The Co(1)−N(3) bond distance (1.906(4) Å) is in accord with a Co−N aryl single bond (1.940 Å).[50] While the N−H hydrogen was located in the Fourier map, a fixed position was used for the structural refinement. The solution magnetic susceptibility of **10** is 3.8 μ_B, in agreement with an $S = {}^3/_2$ ground state. Complexes **10** and **11** were also independently synthesized through the reaction of **2** with LiNHPh and LiNHC$_6$H$_4$CH$_3$, respectively. The yields from the metathesis reactions (72% and 73%, respectively) were much improved compared to

(51) Egan, J. W.; Haggerty, B. S.; Rheingold, A. L.; Sendlinger, S. C.; Theopold, K. H. *J. Am. Chem. Soc.* **1990**, *112*, 2445–2446.
(52) Ingleson, M. J.; Pink, M.; Caulton, K. G. *J. Am. Chem. Soc.* **2006**, *128*, 4248–4249.
(53) Fout, A. R.; Basuli, F.; Fan, H.; Tomaszewski, J.; Huffman, J. C.; Baik, M.; Mindiola, D. J. *Angew. Chem., Int. Ed.* **2006**, *45*, 3291–3295.
(54) Detrich, J. L.; Konecny, R.; Vetter, W. M.; Doren, D.; Rheingold, A. L.; Theopold, K. H. *J. Am. Chem. Soc.* **1996**, *118*, 1703–1712.
(55) Bengali, A. A.; Bergman, R. G.; Moore, C. B. *J. Am. Chem. Soc.* **1995**, *117*, 3879.
(56) Dougherty, T. P.; Heilweil, E. J. *J. Chem. Phys.* **1994**, *100*, 4006.
(57) Rahim, M.; Bushweller, C. H.; Ahmed, K. J. *Organometallics* **1994**, *13*, 4952–4958.
(58) Joslin, F. L.; Johnson, M. P.; Mague, J. T.; Roundhill, D. M. *Organometallics* **1991**, *10*, 2781–2794.
(59) Fagan, P. J.; Manriquez, J. M.; Vollmer, S. H.; Day, C. S.; Day, V. W.; Marks, T. J. *J. Am. Chem. Soc.* **1981**, *103*, 2206–2220.
(60) Ingleson, M. J.; Pink, M.; Fan, H.; Caulton, K. G. *J. Am. Chem. Soc.* **2008**, *130*, 4262–4276.

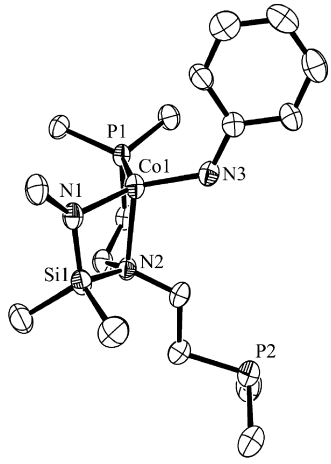

Figure 8. Thermal ellipsoid (50%) plot of **10**. Hydrogen atoms, *iso*-propyl methyl, and *tert*-butyl methyl groups have been omitted for clarity.

Table 10. Selected Bond Lengths (Å) and Angles (deg) for $[N_2P_2]$CoNHPh (**10**)

Co(1)−N(1)	1.908(4)	Co(1)−N(2)	2.241(4)
Co(1)−N(3)	1.906(4)	Co(1)−P(1)	2.3826(17)
N(3)−Co(1)−N(1)	131.49(17)	N(3)−Co(1)−N(2)	109.77(16)
N(1)−Co(1)−N(2)	77.03(16)	N(3)−Co(1)−P(1)	110.18(13)
N(1)−Co(1)−P(1)	118.24(13)	N(2)−Co(1)−P(1)	86.61(11)

those from the reactions of **6** with azide due, we assume, to the absence of side-reactions (see below).

Hydrogen atom abstraction by a transient metal imido species has been reported.[8,61−63] A common test for identifying such reactivity is to carry the reaction out in the presence of 1,2-diphenylhydrazine, which is converted to azobenzene.[61,64] Accordingly, when the reactions of **6** with an arylazides (phenylazide, *p*-tolylazide) were performed in the presence of 0.5 equiv of 1,2-diphenylhydrazine, quantitative conversion of 1,2-diphenylhydrazine to azobenzene was observed by ^{1}H NMR spectroscopy. Compound **6** and phenylazide were also combined in C_6D_6, and the resulting complex was analyzed for deuterium incorporation (Scheme 4). The IR spectrum revealed no N-D band in the expected region (based on reduced mass calculations)—only the N−H absorption at 3320 cm^{-1} was observed. The high resolution EIMS, however, revealed incorporation of deuterium into the *tert*-butyl group of the $[N_2P_2]$ ligand as seen by the change in the molecular ionization peak from 57.1 *m*/*z* (C_4H_9) to 58.1 *m*/*z* (C_4H_8D) when deuterated solvent was used. Similar results have been observed with a related transient Co oxo species supported by the Tp′ (Tp′ = hydridotris(3-*tert*-butyl-5-methylpyrazolylborate) ligand.[51]

In addition to red-orange crystals of **10**, bright green crystals of a second product were isolated following the reaction of **6** with phenylazide. The identity of this material was determined with the aid of an X-ray diffraction study (see Figure 9; Table 11). In forming this product [PhN=P^{i}Pr$_2$-(CH$_2$)$_2$NPh]-[^{t}BuNHSiMe$_2$N(CH$_2$)$_2$P^{i}Pr$_2$]Co (**12**), at least two transformations need to occur on the $[N_2P_2]$ ligand, including oxidation of one of the phosphines by a nitrene group,[10,65] and C−N bond cleavage. The solution magnetic susceptibility of **12** is 4.1 μ_B, in agreement with a high-spin Co(II) center. The yield of **12** was found to be solvent dependent with the highest isolated yield of **12** (15%) obtained using toluene or benzene. A summary of the yields of **10** and **12** in different solvents is provided in Table 12. Analysis of the crude reaction mixture revealed the presence of starting material **6** along with **10** and **12**, in addition to a small quantity of another, unidentified product. The paramagnetic nature of this latter material, its low yield, and poor crystallinity has made identification elusive.

Our data suggest that two competing reactions are operative in the formation of **10** and **12**. The solvent-dependent yields and the deuterium labeling experiment suggest that the formation of **10** involves an imido assisted hydrogen atom abstraction from solvent by the *tert*-butyl group of the ligand (Scheme 5). Examining how the number of equivalents of azide used effects the reaction further supports hydrogen atom abstraction as the route of reduction. Adding 0.5 equiv of phenylazide to **6** led to crude reaction mixtures of **6** and **10**, with no **12** observed. Increasing the amount of azide added to 2 equiv led to reaction mixtures that would not yield crystalline products. Though the yields of **10** and **12** do not follow an obvious trend, they are likely the result of a combination of the solvent polarity and the BDE of available C−H bonds in solution. Under certain conditions (toluene and sufficient amounts of N_3Ph), intramolecular nitrene group transfer is more competitive with hydrogen abstraction, which leads to a higher isolated yield of **12**. When the reaction of **6** and phenylazide is performed in the presence of 1,2-diphenylhydrazine in toluene only **10** is isolated; compound **12** is not observed, further supporting the premise that **12** forms in the absence of sufficient hydrogen-atom donors.

To test whether intermolecular nitrene group transfer reactions could be achieved with intermediate **A**, it was exposed to an atmosphere of CO at −116 °C.[5,11,12,14,16,17] Upon addition of CO, the flask was sealed, and the cold bath was removed. As the flask warmed, the green suspension changed color to yellow. The volatile materials were vacuum-transferred and analyzed by GCMS. Apart from solvent, phenyl-isocyanate was the only other organic product observed, albeit in low yield (30%). Extraction of the remaining yellow solid led to the isolation of **8** in 78% yield. Related attempts to engender nitrene group transfer to other substrates such as alkenes, alkynes, isocyanides, and isocyanates were unsuccessful.

Direct confirmation of complex **A** as a Co(III) imido was hampered by its instability above −70 °C. Our experimental results do, nonetheless, infer the presence of a transient $[N_2P_2]$Co=NAr species. The observed H-atom abstraction to obtain **10** and the nitrene group transfer observed in forming **12** lends support to this notion.

(61) Lucas, R. L.; Powell, D. R.; Borovik, A. S. *J. Am. Chem. Soc.* **2005**, *127*, 11596–11597.
(62) Eckert, N. A.; Vaddadi, S.; Stoian, S.; Lachicotte, R. J.; Cundari, T. R.; Holland, P. L. *Angew. Chem., Int. Ed.* **2006**, *45*, 6868–6871.
(63) Thyagarajan, S.; Shay, D. T.; Incarvito, C. D.; Rheingold, A. L.; Theopold, K. H. *J. Am. Chem. Soc.* **2003**, *125*, 4440–4441.
(64) Harman, W. H.; Chang, C. J. *J. Am. Chem. Soc.* **2007**, *129*, 15128.
(65) Ingleson, M. J.; Pink, M.; Fan, H.; Caulton, K. *J. Am. Chem. Soc.* **2008**, *130*, 4262–4276.

Scheme 4. Formation and Reactivity of a Transient Co(III) Imido

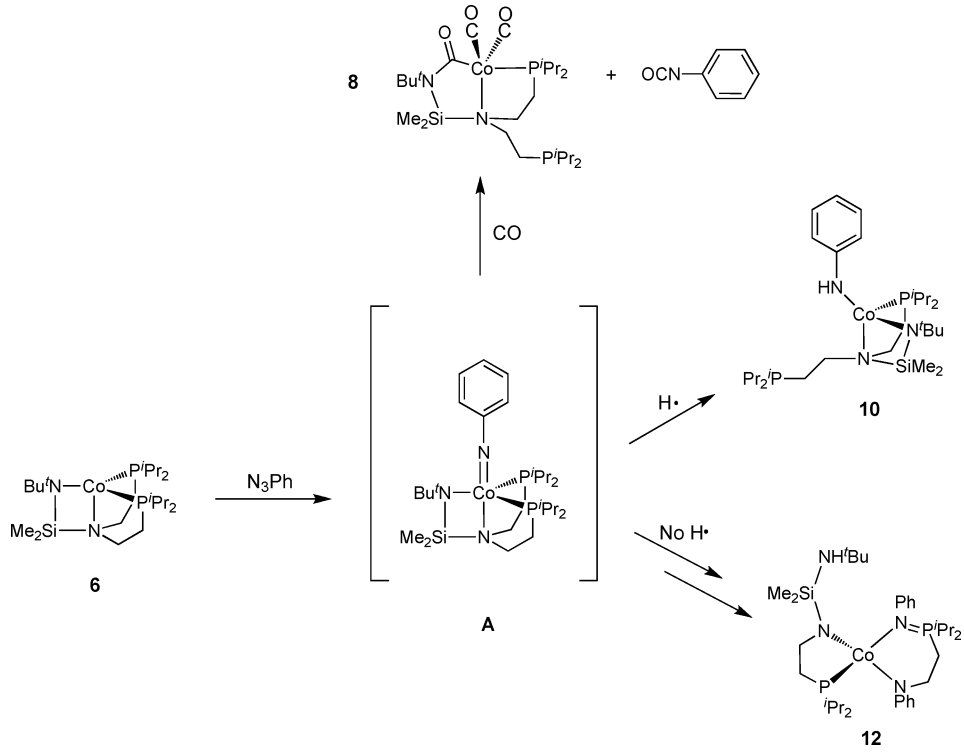

Ligand Modification. With the aim of tuning the reactivity of "[N_2P_2]Co═NAr" to encourage additional group transfer reactions, a modification to the [N_2P_2] ligand was examined in which a *p*-tolyl group replaced the *tert*-butyl functionality.

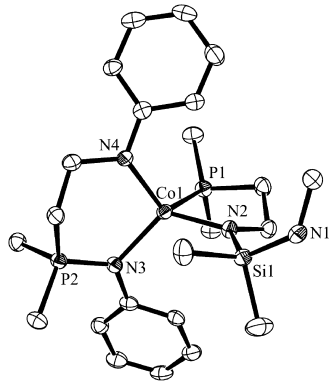

Figure 9. Thermal ellipsoid (50%) plot of **12**. Hydrogen atoms, *iso*-propyl methyl, and *tert*-butyl methyl groups have been omitted for clarity.

Table 11. Selected Bond Lengths (Å) and Angles (deg) for [PhN═P^{i}Pr$_2$(CH$_2$)$_2$NPh][^{t}BuNHSiMe$_2$N(CH$_2$)$_2$P^{i}Pr$_2$]Co (**12**)

Co(1)−N(2)	1.950(2)	Co(1)−N(4)	1.9779(19)
Co(1)−N(3)	2.0694(19)	Co(1)−P(1)	2.4248(8)
P(2)−N(3)	1.619(2)		
N(2)−Co(1)−N(4)	121.02(9)	N(2)−Co(1)−N(3)	119.95(8)
N(4)−Co(1)−N(3)	103.59(8)	N(2)−Co(1)−P(1)	86.90(6)
N(4)−Co(1)−P(1)	114.26(6)	N(3)−Co(1)−P(1)	110.47(6)

Table 12. Solvent Dependent Yields of **10**[a] and **12**[a]

solvent[b]	Yield of **10** (%)	Yield of **12** (%)
pentane	57	<1
toluene	23	15
benzene	20	15
THF	34	7.3

[a] Isolated yield. [b] Approximate BDE (kcal/mol) for pentane (98), toluene (110 and 85), benzene (110), and THF (95).

The *p*-tolyl group was chosen so as to discourage hydrogen atom abstraction from the ligand, thus promoting cleaner nitrene group transfer reactions. The resulting ligand, [$N_2P_2^{tolyl}$], was synthesized in a straightforward manner as follows.

Reaction of Li[PNP] with a slight excess of Cl_2SiMe_2 in pentane resulted in the isolation of ClSiMe$_2$N(CH$_2$CH$_2$P^{i}Pr$_2$)$_2$ (**13**) in quantitative yield. Interaction of **13** with LiNHC$_6$H$_4$CH$_3$ in pentane gave H[$N_2P_2^{tolyl}$] (**14**) in 90% yield following filtration and the removal of solvent under vacuum. Deprotonation of **14** with *n*-BuLi resulted in the formation of Li[$N_2P_2^{tolyl}$] (**15**), which was isolated in 71% yield as a colorless crystalline solid following crystallization from pentane at −40 °C.

Cobalt derivatives with this new [N_2P_2] variant proceeded straightforwardly. Reaction of **15** with CoI_2 in toluene led to the isolation of [$N_2P_2^{tolyl}$]CoI (**16**) as dark brown needles in 80% yield, following crystallization from THF layered with pentane at room temperature. The solution magnetic susceptibility of **16** (4.2 μ_B) indicates the same spin-state as in the *tert*-butyl analogue **2**, and an X-ray diffraction study of **16** revealed a four-coordinate Co center in a distorted tetrahedral geometry similar to that observed in **2**. An ORTEP diagram is shown in Figure 10 with selected bond lengths and angles provided in Table 13. The bond distances observed in **2** and **16** are statistically indistinguishable with the exception of a shorter Co(1)−I(1) bond distance in **16** (2.6916(7) vs 2.7229(7) Å).

Reduction of **16** with KC_8 in DME resulted in a color change of brown to green. Following the removal of solvent under vacuum, extraction with pentane, and cooling at −40 °C, green crystals of [$N_2P_2^{tolyl}$]Co (**17**) were isolated in 84%

Scheme 5. Ligand Assisted H-Atom Abstraction

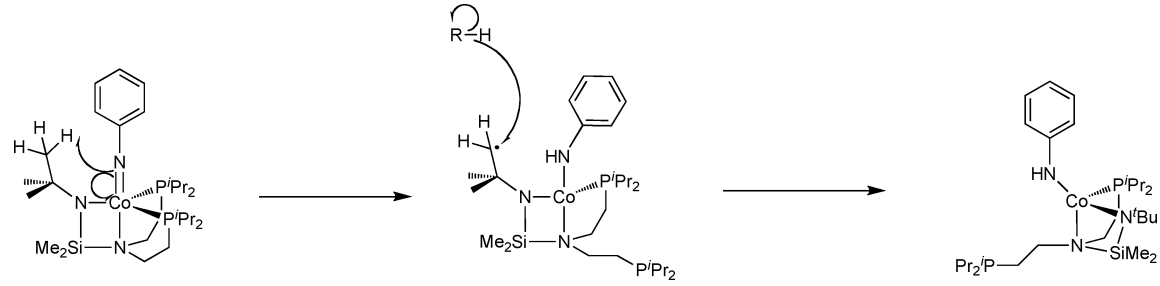

yield. The solid-state structure of **17** was determined by X-ray crystallography, and an ORTEP diagram is shown in Figure 11 with selected bond lengths and angles provided in Table 14. As in **6**, the Co center in **17** lies in a four coordinate trigonal pyramidal geometry with the ligand bound κ^4-N_2P_2, and an open axial coordination site is present. The metal−ligand bond distances in **17** are similar to those observed in **6**, and the solution magnetic susceptibility of **17** is 3.0 μ_B ($S = 1$). As was seen with **16**, compound **6** and **17** possess almost identical geometric parameters.

Exposure of a frozen pentane solution of **17** to 1 equiv of CO resulted in a color change of green to brown and, following the removal of solvent under vacuum, extraction with toluene, concentration, and cooling at−40 °C, brown crystals of the monocarbonyl species [$N_2P_2^{tolyl}$]Co(CO) (**18**) were isolated in 43% yield. One C−O band is present in the IR spectrum (1899 cm^{-1}); the solution magnetic susceptibility is 2.8 μ_B ($S = 1$), similar to compound **7**. The C−O stretching frequencies of the related Co(I) monocarbonyls **7** (1881 cm^{-1}) and **18** (1899 cm^{-1}) indicate that the Co center in **7** is slightly more electron rich and that the [N_2P_2] ligand

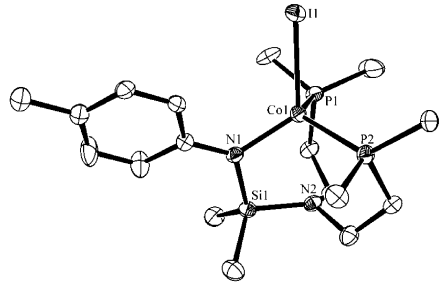

Figure 10. Thermal ellipsoid (50%) plot of **16**. Hydrogen atoms and *iso*-propyl methyl groups have been omitted for clarity.

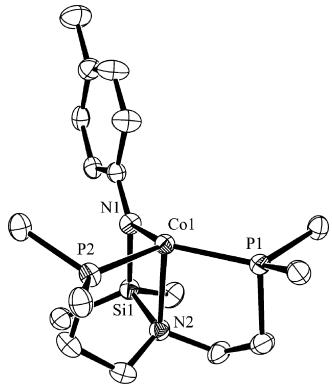

Figure 11. Thermal ellipsoid (50%) plot of **17**. Hydrogen atoms and *iso*-propyl methyl groups have been omitted for clarity.

Table 13. Selected Bond Lengths (Å) and Angles (deg) for [$N_2P_2^{tolyl}$]CoI (**16**)

Co(1)−N(1)	1.958(4)	Co(1)−P(1)	2.3860(14)
Co(1)−P(2)	2.3913(14)	Co(1)−I(1)	2.6916(7)
N(1)−Co(1)−P(1)	107.98(12)	N(1)−Co(1)−P(2)	110.10(12)
P(1)−Co(1)−P(2)	121.00(5)	N(1)−Co(1)−I(1)	118.65(11)
P(1)−Co(1)−I(1)	95.83(4)	P(2)−Co(1)−I(1)	103.23(4)

Table 14. Selected Bond Lengths (Å) and Angles (deg) for [$N_2P_2^{tolyl}$]Co (**17**)

Co(1)−N(1)	1.939(3)	Co(1)−P(2)	2.2077(9)
Co(1)−N(2)	2.216(2)	Co(1)−P(1)	2.2327(8)
N(1)−Co(1)−P(2)	131.90(7)	N(1)−Co(1)−N(2)	78.94(9)
P(2)−Co(1)−N(2)	89.14(6)	N(1)−Co(1)−P(1)	108.87(7)
P(2)−Co(1)−P(1)	117.35(3)	N(2)−Co(1)−P(1)	88.78(6)

Table 15. Electrochemical Data for **2** and **16**

compound	reduction[a,b,c]	oxidation[a,b,c]
2	−1.54V	−0.35 V, 0.08 V
16	−1.47V	0.04 V, 0.42 V

[a] Reported relative to Fc/Fc+. [b] 0.3 M [nBu$_4$N][PF_6] in CH_2Cl_2. [c] 50 mV/s scan rate, non-reversible.

is a slightly better donor than [$N_2P_2^{tolyl}$]. To further probe the electronic differences between complexes supported by [N_2P_2] and [$N_2P_2^{tolyl}$], electrochemical data on the parent metal-halide complexes **2** and **16** were collected. Cyclic voltammograms of these two complexes are similar with both possessing one reductive and two oxidative events in the solvent window (Table 15). The electrochemical data also suggests that the [N_2P_2] ligand in **2** is slightly more electron releasing on the basis of a higher reduction potential and lower oxidation potential as compared to **16**.

Imido Trapping Reactions. As with **6**, a precipitate formed at low temperature (−116 °C) in pentane upon the addition of azide to **17**, and when allowed to warm to room temperature, a color change of green to red-brown was observed. The identity of the resulting complex has yet to be determined because of difficulties in isolating clean material; however, we suspect based on our observations of the reactivity of **6** that a new Co(II) amide might be formed, similar to **10** and **11**. In an effort to detect nitrene functionality, the reactivity of the low temperature species "[$N_2P_2^{tolyl}$]Co=NAr" (Ar = $C_6H_4CH_3$) (**B**), was probed with a number of unsaturated substrates.

As was seen with **A**, addition of an excess of CO to a suspension of **B** resulted in the formation of *p*-tolylisocyanate in 58% yield, as observed by GCMS analysis of the reaction mixture. Also present was a trace quantity of 1,3-di-*p*-tolylcarbodiimide (4% yield). Similarly, the addition of *p*-tolylisocyanide or *p*-tolyl isocyanate to **B** resulted in the formation of 1,3-di-*p*-tolylcarbodiimide in 7% and 8% yield,

respectively. The carbodiimides likely form through nitrene group transfer reactions; however, these reactions appear to be slow compared to the thermal decomposition of **B** based on the low yields of the organic products. Given our inability to isolate any of the metal containing products from these reactions, we cannot definitively say that nitrene group transfer by a transient Co(III) imido is taking place. Nonetheless, given the similarities in the structure and reactivity of **2** and **16** and **6** and **17**, it is reasonable to infer that **A** and **B** would exhibit similar chemistries.

Conclusions

A range of Co complexes supported by $[N_2P_2]$ ligands have been explored. Complexes **3**−**5** demonstrate the robustness of the $[N_2P_2]$ ligand toward reactive Co−C and Co−H functional groups. A common feature of this ligand set is again evidenced in its Co chemistry, namely the coordination mode of the $[N_2P_2]$ framework can change to accommodate steric and electronic demands of the metal center. A low-valent Co(I) compound supported solely by the $[N_2P_2]$ ligand possessing an open axial coordination site was also isolated, and its reactivity with a number of small molecules was probed. Changes in reactivity in select Co complexes was probed following the replacement of the *tert*-butyl group on the anionic nitrogen of $[N_2P_2]$ with a *p*-tolyl group. Though only minor changes were observed in the structural features of the resulting complexes, increased nitrene group transfer reactions were achieved.

Acknowledgment. We are grateful to the National Science Foundation for financial support for parts of this work and Dr. Fred Hollander and Dr. Antonio DiPasquale for crystallographic assistance.

Supporting Information Available: Crystallographic information files (CIFs). This material is available free of charge via the Internet at http://pubs.acs.org.

IC802337T